Astron. Astrophys. 347, 401–408 (1999)

ASTRONOMY AND ASTROPHYSICS

Radiative losses of optically thin coronal plasmas

E. Landi and M. Landini

Department of Astronomy and Space Science, University of Florence, Italy

Received 9 March 1999 / Accepted 6 May 1999

Abstract. In the present work the total radiative losses and the total emissivity curve are calculated for an optically thin plasma using the Arcetri Spectral Code in the 10^4–10^8 temperature range. Checks have been made on the effects of changes in the parameters involved in the calculations, such as element abundances, ion fractions, electron density and transition probabilities on the resulting curves. Parametric fits are given for the resulting radiative losses curves and comparison is made with previous results.

Key words: plasmas – radiation mechanisms: non-thermal

1. Introduction

Radiative losses are a fundamental physical process taking place in plasmas, and their knowledge is essential to evaluate the plasma energy balance and build up models of the source.

In the past, several calculations have been performed by many authors including both continuum and line emission for an increasing number of ions: Cox & Tucker 1969 and Tucker & Koren 1971, later used by Landini & Monsignori Fossi 1975 for loop modeling; McWhirter et al. 1975 also providing analytical fits to their results, Raymond 1979, used by Rosner et al. 1978 for loop modeling, Summers & McWhirter 1979, Gaetz & Salpeter 1983, Landini & Monsignori Fossi 1990, Sutherland & Dopita 1993 and many others.

The calculation of this function requires the knowledge of a large amount of atomic data and transition probabilities for both line and continuum radiation. Each of these calculations used state-of-the-art datasets of transition probabilities, but in the last few years many new and more accurate calculations of atomic data have become available for a large number of ions of the most abundant elements. Also, these calculations evaluated level populations using the *Coronal Model Approximation*. The use of new transition probabilities and the evaluation of detailed atomic level population may change the radiative losses and affect the energy balance.

Recently large databases such as CHIANTI (Dere et al. 1997, Landi et al. 1999) and ADAS (Summers et al. 1996) have been created including the most accurate transition probabilities available in the literature, thus enabling a complete recalculation of the radiative losses. In the present work we have made use of the Arcetri Spectral Code (Landi & Landini 1998, described in Sect. 2) to calculate line and continuum radiation in order to evaluate the total emissivity and the radiative losses for an optically thin plasma. The results are presented in Sect. 3.

As line and continuum radiation depends on a number of parameters such as electron density, ion fractions, element abundances and atomic models, Sect. 3 also reports a critical discussion on the effects of changes in each of these parameters on the resulting radiative losses. Parametric fits are given to the resulting radiative losses curves in Sect. 4 which may help the analytical integration of theoretical models.

Send offprint requests to: E.Landi (enricol@arcetri.astro.it)

2. Theoretical calculations

The energy emitted by an optically thin plasma per unit volume, wavelength and time may be expressed as

$$I_{rad}(\lambda, T, N_e) = \varepsilon(\lambda, T, N_e)\ N_e^2 \qquad erg\ cm^{-3}\ s^{-1}\ \text{Å}^{-1} \quad (1)$$

where $\varepsilon(\lambda, T, N_e)$ is the plasma emissivity, given by

$$\varepsilon(\lambda, T, N_e) = G_{line}(\lambda, T, N_e) + G_{cont}(\lambda, T, N_e) \quad (2)$$

$G_{cont}(\lambda, T, N_e)$ is the continuum *Contribution Function*; $G_{line}(\lambda, T, N_e)$ is the sum of all the single line *Contribution Function* found in the selected wavelength band. Each line *Contribution Function* is given (in erg cm^3 s^{-1}) by

$$G(T, \lambda_{i,j}) = \frac{N_j(X^{+m})}{N(X^{+m})} \frac{N(X^{+m})}{N(X)} \frac{N(X)}{N(H)} \frac{N(H)}{N_e} \frac{A_{ji} h\nu_{ij}}{N_e} \quad (3)$$

where

- $\frac{N_j(X^{+m})}{N(X^{+m})}$ is the relative upper level population of the ion X^{+m};
- $\frac{N(X^{+m})}{N(X)}$ is the relative abundance of the ion X^{+m};
- $\frac{N(X)}{N(H)}$ is the abundance of the element X relative to Hydrogen;
- $\frac{N(H)}{N_e}$ is the hydrogen abundance relative to the electron density (≈ 0.8);

The total radiated energy per unit volume and time E_{rad} lost by the plasma is then given by the sum of the emission at all wavelengths:

$$\frac{E_{rad}}{dV dt} = \int_\lambda \varepsilon(\lambda, T, N_e)\ N_e^2\ d\lambda \qquad erg\ cm^{-3}\ s^{-1} \quad (4)$$

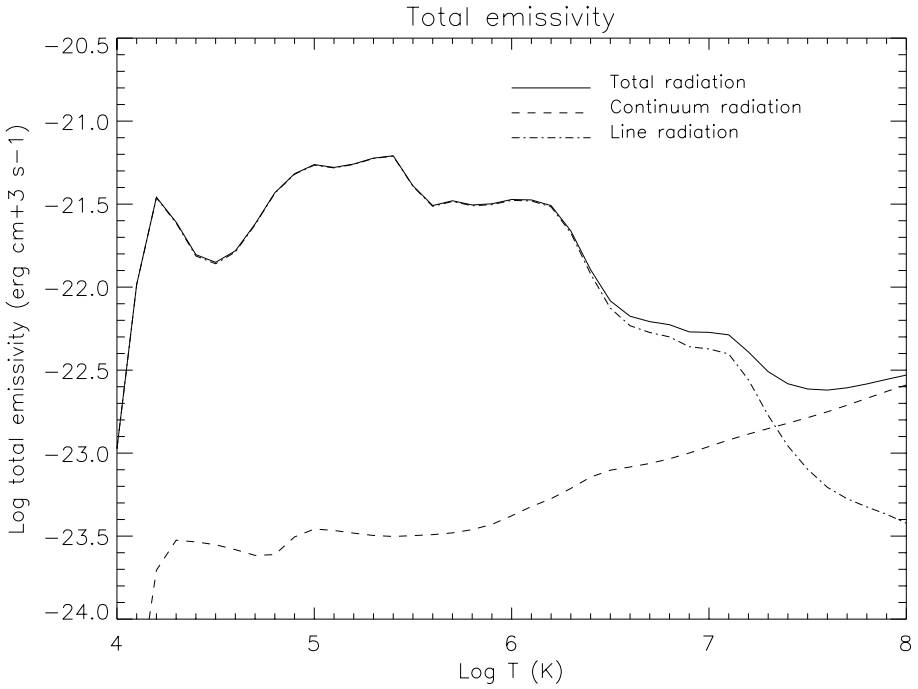

Fig. 1. Total radiated power per unit $N_e^2\ dV$ as a function of electron temperature, calculated at $N_e = 10^{10}$ cm^{-3}.

while the total radiated power per unit $N_e^2 dV$ (total emissivity) of the emitting plasma is given by

$$\eta(T, N_e) = \frac{E_{rad}}{N_e^2 dV dt} = \int_\lambda \varepsilon(\lambda, T, N_e)\, d\lambda \quad erg\ cm^3\ s^{-1} \quad (5)$$

Here a brief description of the Arcetri Code is given, for further details the reader is referred to the quoted paper.

The Arcetri Code consists of a set of routines and a database of atomic parameters and transition probabilities necessary to calculate line and continuum emission from an optically thin plasma. The continuum radiation is evaluated according to Landini & Monsignori Fossi 1990 including free-free, free-bound and two-photon processes. Line radiation is calculated for most of the ions of astrophysical interest using two different approximations: *(a)* solving the statistical equilibrium equations for ion level population or *(b)* using the *Coronal Model Approximation*. The Arcetri Code covers the 1–2000 Å spectral range, and calculates line emission for approximately 175 ions. The atomic data and transition probabilities database necessary for using method *(a)* is the same as for the CHIANTI project (Dere et al. 1997, Landi et al. 1999).

The calculation of the theoretical spectrum of an optically thin plasma depends on a number of parameters: electron density, element abundances, ion fractions, atomic data and transition probabilities for the calculation of level populations for the emitting ions. In the present work we investigate the effects of these parameters in the resulting radiative losses. For this reason we have calculated the theoretical spectrum for several values of the electron density (10^8, 10^{10}, 10^{12}, 10^{14} cm^{-3}), using different sets of element abundances (Allen 1973, Feldman 1992, Grevesse & Anders 1991, Meyer 1985 and Waljeski 1994) and ion fraction calculations (Shull & Steenberg 1982, Arnaud & Rothenflug 1985, Arnaud & Raymond 1992, Mazzotta et al. 1998) under the assumption of ionization equilibrium. Also, in order to assess the improvement of the new dataset of atomic parameters and transition probabilities on the radiative losses curves we have performed a comparison between the present results and those obtained with and old version of the Arcetri Code found in Landini & Monsignori Fossi 1990.

3. Results

An example of the total emissivity curve as resulting from the present version of the Arcetri Code calculation is displayed in Fig. 1. It has been evaluated assuming $N_e = 10^{10}$ cm^{-3} and adopting the Arnaud & Raymond 1992 (Fe ions) and Arnaud & Rothenflug 1985 (other ions) ion fractions and the Feldman 1992 element abundances. The calculation has been performed for temperatures in the 10^4–10^8 K range, but it is important to note that for temperatures smaller than 10^5 K opacity effects play an important role in line and continuum radiation formation. As these effects are not accounted for in the present calculation, the total emissivity curve and the radiative losses curves should be taken with caution below this temperature limit.

Fig. 2 shows the contribution of the most abundant elements to the total emissivity curve. Hydrogen is responsible for nearly all the radiative losses at chromospheric temperatures, while iron provides most of the output energy at high temperature. Continuum radiation may be neglected for all temperatures lower than a few million degrees, but at very high temperature free-free continuum radiation dominates the total emissivity.

Figs. 3 and 4 display the total emissivity for some of the most abundant elements in astrophysical plasmas together with the strongest lines of each of the element's ions. For some temperatures the total emissivity of some elements is dominated by the emission of a very small number of very strong lines; these

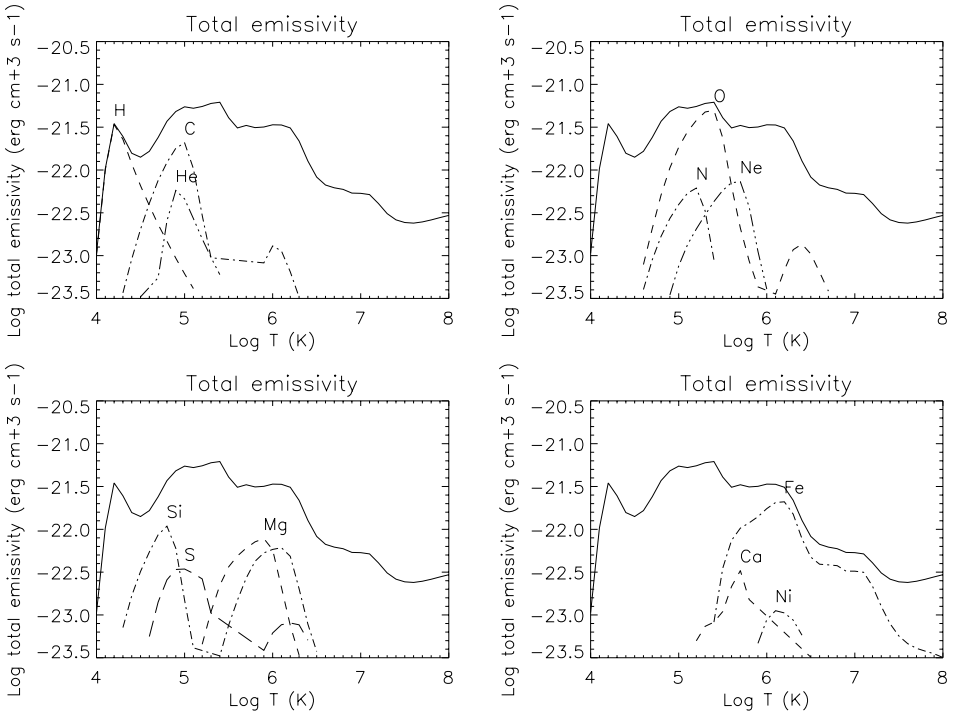

Fig. 2. Contribution of the most abundant elements to the total emissivity curve.

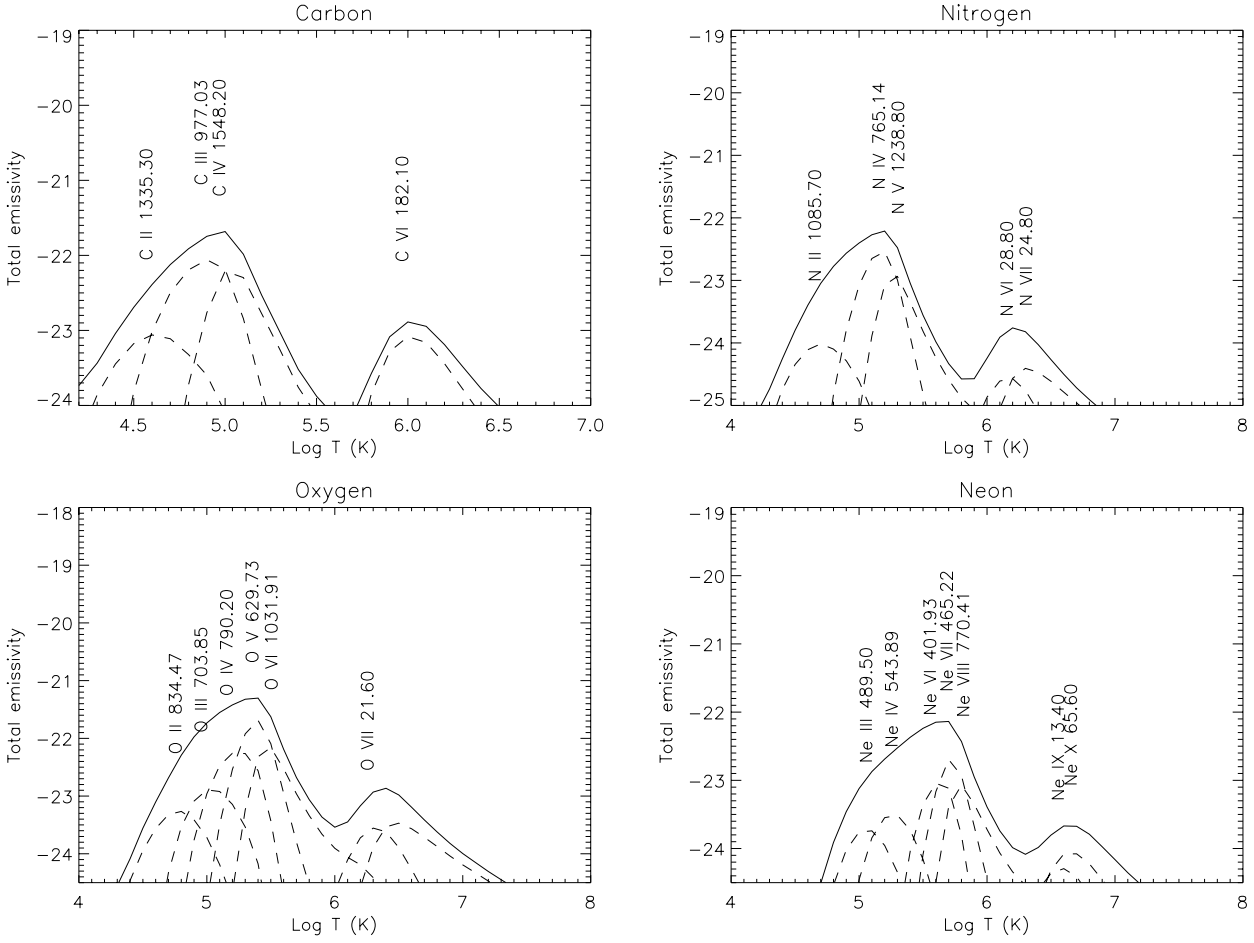

Fig. 3. *Contribution Function* of the strongest line of each ion to the total emissivity of the most abundant elements.

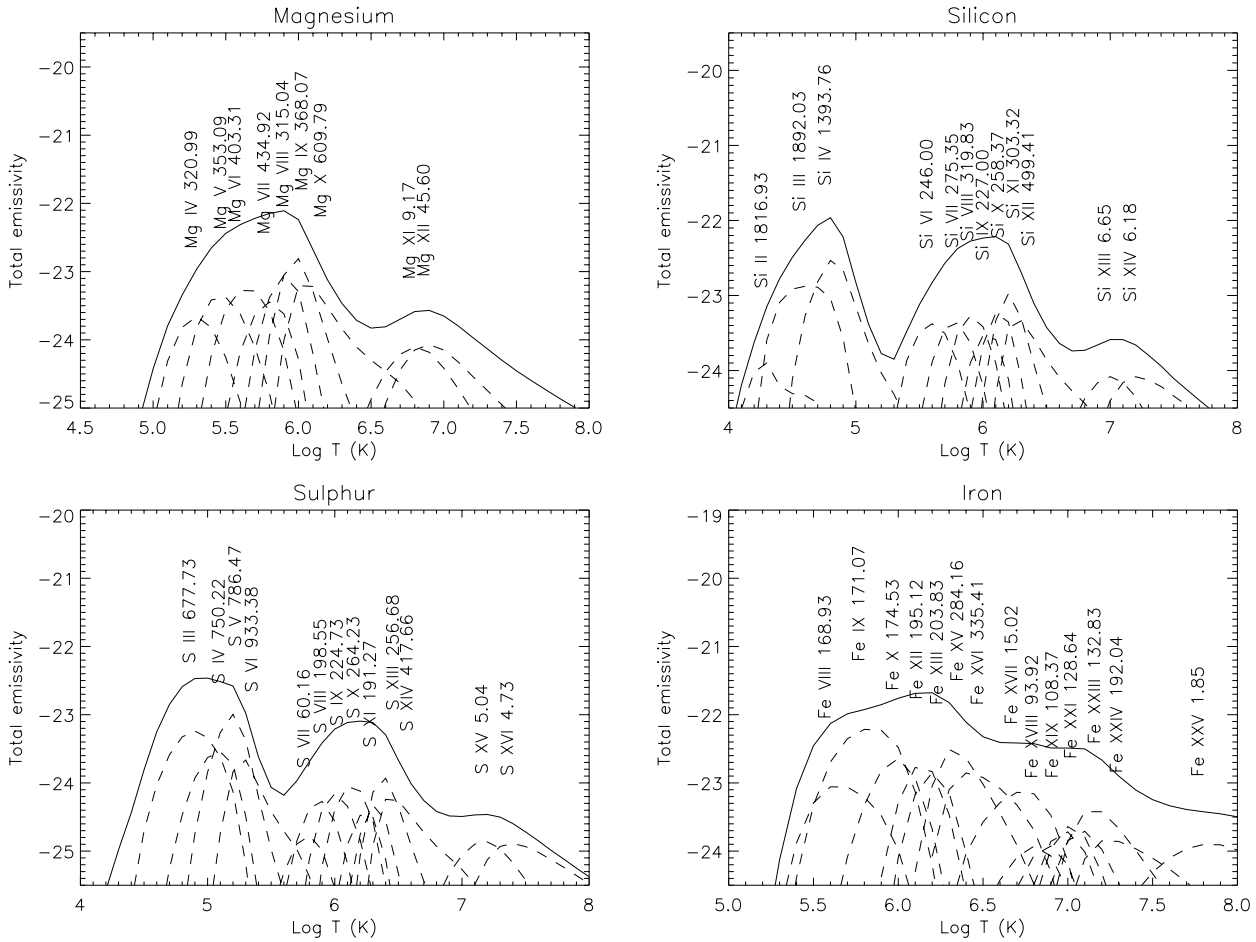

Fig. 4. *Contribution Function* of the strongest line of each ion to the total emissivity of the most abundant elements.

are some of the strongest spectral features observed in solar and stellar spectra.

3.1. Effect of the electron density

Both continuum and line radiation may be electron density dependent, and this may cause the radiative losses and the total emissivity curve to be density dependent as well. As in literature the total emissivity curve is usually given as a function of temperature only, it is important to check the density dependence of this curve.

Continuum radiation electron density dependence stems from the two-photons continuum process: the populations of the H-like $2s^2$S level and of the He-like $1s2s^1$S level, decaying to the ground level through a two-photon process, may be altered by collisional de-excitation when electron density reaches a critical value. However the two-photons continuum represents a minor contribution to the continuum radiation at coronal densities and temperatures. Line radiation electron density dependence is given by the role played by collisional excitation and de-excitation into level population; this dependence may provide precious diagnostic tools for determining the electron density of the emitting plasma. Another source of density dependence is given by density effects on ionization and recombination coefficients. Summers 1972 and 1974 calculated density-dependent ionization equilibrium finding that ion fractions change as a function of density, mostly because of the density dependence of the dielectronic recombination coefficient; Vernazza & Raymond 1979 also find that under coronal condition ion fractions are density dependent, mostly due to collisional ionization and dielectronic recombination. Plasma microfields also may have a significant effect on dielectronic recombination, giving a further density dependence to ion fractions. Badnell et al. 1993 carried out quantal calculations for dielectronic recombination of C IV in an electric field, finding that the dielectronic recombination rate could change by 40%.

However, in the literature ion fractions are usually reported as a function of electron temperature only, so in the present work it is not possible to check the effects of their density dependence on the total emissivity curve due to ionization balance.

In order to assess the density dependence due to level population we have performed the theoretical calculation of this curve assuming four different values of the electron density: 10^8, 10^{10}, 10^{12}, 10^{14} cm^{-3}. Outside this density range line radiation is density insensitive: for higher densities ion level populations for the most important lines have reached Boltzmann

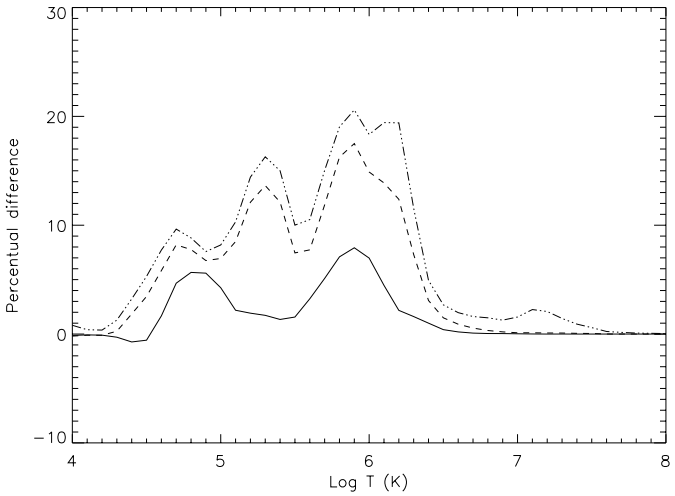

Fig. 5. Percentual differences between total emissivity curves calculated assuming different values of the electron density. *Full line*: 10^8 vs. 10^{10} cm^{-3}; *Dashed line*: 10^8 vs. 10^{12} cm^{-3}; *Dash-dotted line*: 10^8 vs. 10^{14} cm^{-3}.

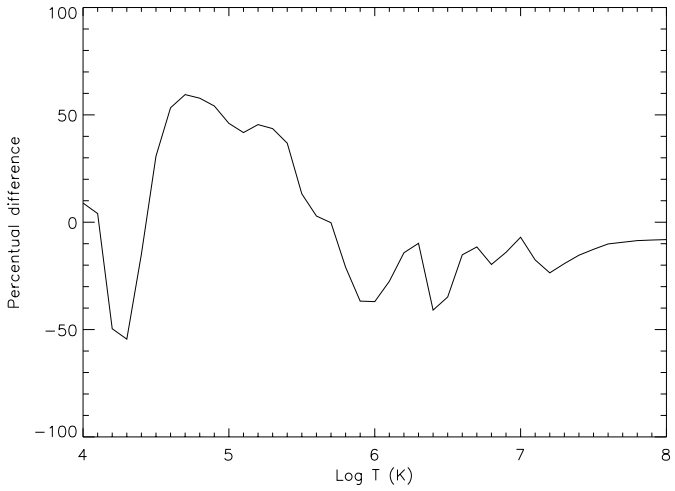

Fig. 6. Percentual difference between the total emissivity curve obtained with the old and new version of the Arcetri Spectral Code. The adopted electron density is 10^{10} cm^{-3}.

equilibrium, while for lower densities collisional de-excitation becomes negligible compared to radiative decay and the *Coronal Model Approximation* (yielding density insensitive line *Contribution Functions*) may be adopted.

Fig. 5 displays the percentual difference

$$Perc.\ Diff(i) = \frac{\eta\big(T, N_e = 10^8\big) - \eta\big(T, N_e^i\big)}{\eta(T, N_e = 10^8)} \qquad (6)$$

(with $N_e^i = 10^{10}, 10^{12}$ and 10^{14} cm^{-3}) between total emissivity curves calculated at different densities as a function of electron temperature. As expected, the greatest differences are found with the curves at $10^{12} - -10^{14}$ cm^{-3}, which are very similar, because density-dependence affects line emissivity mostly between 10^8 and 10^{10} cm^{-3}. Differences are always smaller than 25% and show a marked temperature dependence, being highest at transition region and coronal temperatures and decreasing down to zero at the edges of the selected temperature range.

The maximum at coronal temperatures is given by the presence of a host of strong density dependent lines formed in quiet corona, mainly from Fe, Mg and Si ions. The high temperature tail is dominated by strong, density insensitive lines and free-free continuum; the low temperaure tail is dominated by density insensitive transition region and chromospheric lines and for this reason there are small differences between computations carried out assuming different density values.

3.2. Effect of different datasets and approximations in level population computation

Level populations are strongly sensitive to any change or problem in the atomic parameters, collision strengths and transition probabilities as well as in the approximation adopted for their calculations, and this affects line radiation. It is therefore important to check the effects of different transition probabilities datasets on the resulting total emissivity curve.

As big improvements have been done in the present version of the Code versus the older version described in Landini & Monsignori Fossi 1990, we have performed a comparison between the present results and those obtained using the 1990 version of the Arcetri Code. The adopted element abundances are from Allen 1973. There are three main differences between the two versions of the Arcetri Code: *(a)* the old 1990 Code calculated *all* line intensities using the *Coronal Model Approximation, (b)* the collision rates were calculated using Gaunt factors and *(c)* radiative data came from different literature sources than in the present version of the Code.

Thus, the present comparison allows to check also the effects of different assumptions in level population calculations on the resulting total plasma emissivity.

Fig. 6 displays the percentual difference

$$Perc.\ diff = \frac{\eta_{old} - \eta_{new}}{\eta_{old}} \qquad (7)$$

between the two versions of the Code as a function of electron temperature. It is possible to see that rather high differences (up to 60%) are found at transition region temperatures, and smaller discrepancies occur at coronal temperatures. In the positive section of Fig. 6 the older version of the Arcetri Code has higher total emissivity than the more recent version at transition region temperatures. This is due to the presence of few very bright transitions from O IV, O V, C IV whose emissivities have very different values in the two versions of the Code; their difference is due both to the use of different datasets and to the different approximations used in level population calculation leading to an overestimation of line emissivity for these transitions in the old version of the Code. The negative section of the diagram is due to the much larger number of lines included in the new version.

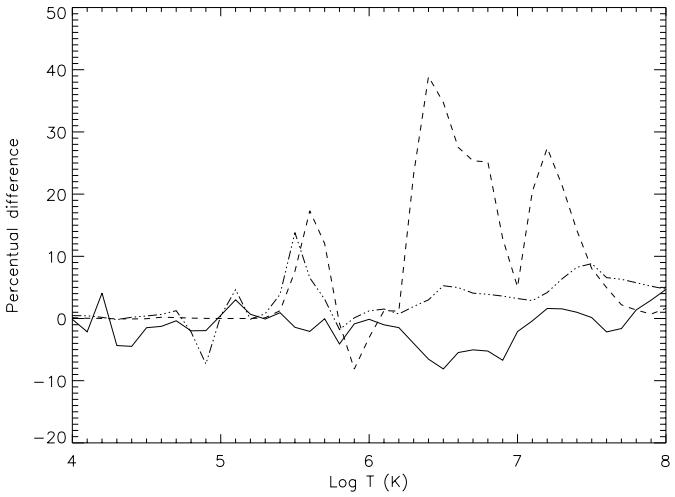

Fig. 7. Percentual difference between total emissivity obtained with RA ion fractions and: *Full line*: MA ion fractions; *Dashed line*: RO ion fractions; *Dash-dotted line*: SS ion fractions. The adopted electron density is 10^{10} cm^{-3}, element abundances are from Feldman 1992.

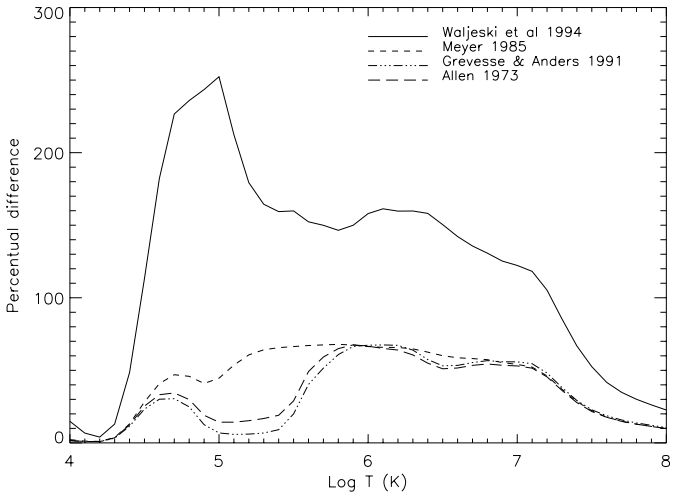

Fig. 8. Percentual difference between total emissivity obtained adopting Feldman 1992 abundances and those obtained with Allen 1973, Grevesse & Anders 1991, Meyer 1985 and and Waljeski et al. 1994 datasets.

3.3. Effect of ionization equilibrium

Ion fractions are necessary to both line and continuum calculation and any difference in their values are usually reflected into the total emissivity curve. We have checked the changes between curves calculated adopting different ion fractions datasets. All these calculations have been carried out assuming ionization equilibrium, and ion fractions come from Shull & Steenberg 1982 (SS, but with H and He ion fractions coming from Arnaud & Rothenflug 1985), Arnaud & Rothenflug 1985 (RO), Arnaud & Rothenflug 1985 plus Arnaud & Raymond 1992 for the Fe ions (RA), Mazzotta et al. 1998 (MA).

Fig. 7 displays the percentual differences

$$Perc.\ diff(i) = \frac{\eta_{RA} - \eta_i}{\eta_{RA}} \tag{8}$$

between the results obtained adopting RA ion fractions and those obtained with the other three datasets. The overall differences are smaller than 40%, and the greater differences are found with RO ion fractions. These are due to Fe ion fractions, dominating the high temperature tail of the total emissivity curve (the other elements' ion fractions being the same). Differences with the SS and MA results are much smaller.

On the overall, the effect of the use of different ion fractions onto the total emissivity curve may rise up to a maximum of 40%, and are smaller than 20% at transition region and chromospheric temperatures below 10^6 K.

3.4. Effect of element abundances

Variation of the chemical composition of the emitting plasma may change the total emissivity curve by very large amounts.

It has been long acknowledged that element abundances change in solar plasmas, and their values seem to be associated to magnetic structures in the solar atmosphere (see the reviews of Feldman et al. 1992, Feldman 1992, Mason 1995). These variations seem to be related to the First Ionization Potential (FIP) of the emitting elements (e.g. Haisch et al. 1996). Cook et al. 1989 determined the radiative loss function using photospheric, chromospheric and coronal abundaces and found huge differences in the 10^5–10^6 K temperature range; they also found that these changes have serious effects on loop models.

Also Böhringer & Hensler 1989 and Sutherland & Dopita 1993 have studied the effects of metallicity variations on total emissivity curve, finding huge differences as metallicity decreases from the solar value. This is due to the importance of line radiation from elements with $Z \geq 6$ at temperatures between 10^5 and 10^7 K.

The importance of abundance changes pointed out by these authors has led us to check the effect of different element abundance values on the resulting total emissivity curve. As this curve is dominated by the emission of some elements, these effects are expected to be very large. In order to check these effects total emissivities have been calculated assuming several different sets of element abundances: Allen 1973 (AL), Feldman 1992 (FE), Grevesse & Anders 1991 (GA), Meyer 1985 (ME) and Waljeski et al. 1994 (WA).

Fig. 8 displays the percentual differences

$$Perc.\ diff(i) = \frac{\eta_{FE} - \eta_i}{\eta_{FE}} \tag{9}$$

Table 1. Fit coefficients for the parametric curve in Eq. 11. a_n values are reported in Table 2.

Abund.	α	β	n_{max}	Accuracy
FE	33.64	2.56	8	20%
AL	33.92	2.53	10	16%
GA	33.89	2.55	8	25%
ME	34.06	2.43	9	13%
WA	33.24	2.68	9	16%

Table 2. Fit coefficients for the parametric curve in Eq. 11. α, β and n_{max} values are reported in Table 1.

Abund.	a_n										
	a_0	a_1	a_2	a_3	a_4	a_5	a_6	a_7	a_8	a_9	a_{10}
FE	1.06	−2.39	9.16	−10.1	4.99	−1.29	0.182	-1.30×10^{-2}	3.74×10^{-4}		
AL	1.58	−10.6	35.9	−50.7	37.7	−16.5	4.49	−0.765	7.91×10^{-2}	-4.54×10^{-3}	1.10×10^{-4}
GA	1.49	−6.59	15.2	−14.3	6.72	−1.70	0.235	-1.67×10^{-2}	4.78×10^{-4}		
ME	1.43	−8.57	28.2	−35.2	22.0	−7.68	1.57	−0.187	1.19×10^{-2}	-3.12×10^{-4}	
WA	1.05	−3.25	16.6	−23.6	15.5	−5.57	1.16	−0.139	8.86×10^{-3}	-2.33×10^{-4}	

found between the emissivity curve calculated using FE abundances and those calculated adopting the other datasets. There are huge variations (up to a factor 2.5) between FE and WA total emissivities, while differences up to 70% are found between FE and the other three sets of abundance values.

Considering the results shown in Fig. 8, and that differences up to factor 9 have been observed in the solar atmosphere between distinct structures very close to each other (e.g. Young & Mason 1997), abundance variations are a key factor for the evaluation of total plasma emissivity and need to be carefully chosen in order to be able to properly determine the plasma radiative losses.

4. Parametric fit of the results

Radiative losses are a key parameter for the energy balance of any plasma, and threfore it is very important to accurately know their temperature dependence. Some of these models may be integrated analytically and a parametric fit of the radiative losses may prove useful in this case. For this reason parametric fit have been determined for the radiative losses curve resulting from the present calculations.

The adopted ion fractions come from Arnaud & Raymond 1992 (Fe ions), Arnaud & Rothenflug 1985 (other ions) and Landini & Monsignori Fossi 1991 for the Minor Ions. The electron density is $N_e = 10^{10}$ cm^{-3}. As element abundances cause huge variations to the total emissivity curve (and hence to the total radiated power), parametric fits have been calculated for each of the element abundance sets checked in Sect. 3.4.

The quantity

$$E_{rad}\ \frac{4k^2}{P_0^2} = \frac{\eta(T, N_e)}{T^2} \qquad erg\ cm^3\ s^{-1}\ K^{-2} \tag{10}$$

has been considered and it has been approximated as

$$E_{rad}\ \frac{4k^2}{P_0^2} = 10^{-\alpha} \left(\frac{T}{10^6}\right)^{-\beta} \Sigma_{n=0}^{n_{max}}\ a_n \left(\frac{T}{10^6}\right)^{-n} \tag{11}$$

Values for α, β, n_{max} and a_n are reported on Tables 1 and 2 for each of the element abundances datasets. T is in K, P_0 is in dyne and E_{rad} is in erg cm^{-3} s^{-1}. Table 1 also reports the average accuracy of the fitted curve to the original $E_{rad}\ \frac{4k^2}{P_0^2}$ curve. This formula is given for temperatures in the 10^5-10^8 K range. We have not included in the parametric fit radiative losses for temperature smaller than 10^5 K because at these temperatures opacity effects (not accounted for in the present calculation) are significant, and they lead to alterations into the radiative losses curves.

5. Discussion and conclusions

In this paper the total radiative losses and the total emissivity curves have been calculated for optically thin plasmas in the temperature range 10^4-10^8 K using the new version of the Arcetri Spectral Code.

These two curves have been calculated using different datasets for element abundances, ion fractions, transition probabilities and adopting several values of the electron density. The comparison between the resulting curves allows to evaluate the effects of each of these parameters on the total radiative losses and the total emissivity.

Parametric fits have been determined for the results; these fits may be used for analytical solution of models for the energy balance of the emitting plasma.

The total emissivity curves resulting from the present computation have been compared also with some parametric fit of total emissivity curves found in literature. The comparison has been carried out with the parametric fit given by Landini & Monsignori Fossi 1975 and Rosner et al. 1978. The latter parametric fit has been extensively used for loop modeling throughout the years. The parametric fit given by Rosner et al. 1978, based on a detailed calculation by Raymond 1979 agrees with the present results better than 50% for temperatures smaller than $10^{6.3}$ K. On the contrary the too simple approximation used by Landini & Monsignori Fossi 1975 shows big differences with the present results.

Acknowledgements. We acknowledge the financial support from the Italian Ministry of University and Technological Development (MURST contract 40% 1996); EL acknowledges financial support from the Italian Space Agency (ASI contract RS-96.141). We would like to thank the referee, Dr. J.C. Raymond, for very useful comments on the original manuscript.

References

Allen C.W., 1973, Astrophysical Quantities. The Athlone Press, London, p. 31
Arnaud M., Raymond J.C., 1992, ApJ, 398, 394
Arnaud M., Rothenflug R., 1985, A&AS 60, 425
Badnell N.R., Pindzola M.S., Dickson W.J., et al., 1993, ApJ 407, L91
Böhringer H., Hensler G., 1989, A&A 215, 147
Cook J.W., Cheng C.-C., Jacobs V.L., Antiochos S.K., 1989, ApJ 338, 1176

Cox D.P., Tucker W.H., 1969, ApJ 157, 1157
Dere K.P., Landi E., Mason H.E., Monsignori Fossi B.C., Young P.R., 1997, A&AS 125, 149
Feldman U., 1992, Physica Scripta 46, 202
Feldman U., Mandelbaum P., Seely J.F., Doscheck G.A., Gursky H., 1992, ApJS 81, 387
Gaetz T.J., Salpeter E., 1983, ApJS 52, 155
Grevesse N., Anders E., 1991, In: Cox A.N., Livingston W.C., Matthews M.S. (eds.) Solar Interior and Atmosphere. Univ. Arizona Press, Tucson, 1227
Haisch B., Saba J.L.R., Meyer J-P., 1996, In: Pallavicini R., Dupree A.K. (eds.) Proceedings of the 9^th Cambridge Workshop on Cool Stars, Stellar Systems and the Sun. ASP Conf Series 109, p. 511
Landi E., Landini M., 1998, A&AS 133, 411
Landi E., Landini M., Dere K.P., Young P.R., Mason H.E., 1999, A&AS, in press
Landini M., Monsignori Fossi B.C., 1975, A&A 42, 213
Landini M., Monsignori Fossi B.C., 1990, A&AS 82, 229
Landini M., Monsignori Fossi B.C., 1991, A&AS 91, 183
Mason H.E., 1995, Adv. Space. Res. 15(7), 53
Mazzotta P., Mazzitelli G., Colafrancesco S., Vittorio N., 1998, A&AS 133, 403
McWhirter R.W.P., Thonemann P.C., Wilson R., 1975, A&A 40, 63
Meyer J.P., 1985, ApJS 57, 173
Raymond J.C., 1979, unpublished calculations
Rosner, R., Tucker W.H., Vaiana G.S., 1978, ApJ 220, 643
Shull J.M., Van Steenberg M., 1982, ApJS 48, 95
Summers H.P., 1972, MNRAS 158, 255
Summers H.P., 1974, MNRAS 169, 663
Summers H.P., McWhirter R.W.P., 1979, J. Phys. B 12, 2387
Summers H.P., Brooks D.H., Hammond T.J., Lanzafame A.C., Lang J., 1996, RAL Technical Report RAL-TR-96-017, March 1996
Sutherland R.S., Dopita M.A., 1993, ApJS 88, 253
Tucker W.H., Koren M., 1971, ApJ 168, 283
Vernazza J.E., Raymond J.C., 1979, ApJ 228, L89
Young P.R., Mason H.E., 1997, Solar Physics 175, 523
Waljeski K., Moses D., Dere K.P., et al., 1994, ApJ 429, 909